Effect of Medium pH on the Reactivity Ratios in Acrylamide Acrylic Acid Copolymerization

A. Paril,[1] A. M. Alb,[2] A. T. Giz,[1] H. Çatalgil-Giz[1]

[1]*İ.T.Ü. Fen-Edebiyat Fakültesi, 34469 Maslak, Istanbul, Türkiye*
[2]*Physics Department, Tulane University, Stern Hall, New Orleans, Louisiana 70118*

Received 1 June 2006; accepted 13 July 2006
DOI 10.1002/app.25271
Published online in Wiley InterScience (www.interscience.wiley.com).

ABSTRACT: The copolymerization reactivity ratios of acrylic acid and acrylamide are found at pH 5 and pH 2. Automatic continuous online monitoring of polymerization reactions (ACOMP) has been used for the first time to monitor the synthesis of polyelectrolytic copolymers. The composition drift during the reactions revealed that at pH 5, the acrylamide participates more in the copolymer, and at pH 2, the acrylic acid incorporates in the system at a higher ratio. The copolymerization data were analyzed by a recent error in variables (EVM) type calculation method developed for obtaining the reactivity ratios by on-line monitoring and gave at pH 5 reactivity ratios $r_{\mathrm{Aam}} = 1.88 \pm 0.17$, $r_{\mathrm{Aac}} = 0.80 \pm 0.07$ and at pH 2 $r_{\mathrm{Aam}} = 0.16 \pm 0.04$, $r_{\mathrm{Aac}} = 0.88 \pm 0.08$. The results show that the reactivity ratios depend strongly on the pH of the medium. The effect of polyelectrolytic interactions on the reactivity ratios is discussed in detail. © 2006 Wiley Periodicals, Inc. J Appl Polym Sci 103: 968–974, 2007

Key words: polyelectrolytes; copolymerization; reactivity ratios; water-soluble polymers

INTRODUCTION

The properties of polyelectrolytes have been studied experimentally, theoretically, and computationally for many years.[1] Behind these studies lies the fundamental fact that most biopolymers are polyelectrolytes (including polyampholytes), and that synthetic polyelectrolytes have a variety of uses in diverse industries.

The monomers of polyelectrolytes are usually expensive and difficult to polymerize. For this reason, polyelectrolytes are commonly used in the form of copolymers with cheaper and more easily obtainable nonionic comonomers. Another reason for this usage is that the polyelectrolytic effects depend on the linear charge density of the molecule, which is limited by counterion condensation to one unit per Bjerrum length. The Bjerrum length is 0.72 nm at room temperature in water. The length of a monomeric unit is about 0.25 nm, and it is not effective to place the charged groups closer than a Bjerrum length; approximately two uncharged units should be placed between two charged groups. Thus, chains of maximum hydrodynamic volume can most economically and easily obtained by copolymerization of charged and uncharged monomers, namely copolyelectrolytes.

Here, the copolymerization reactivity ratios of acrylamide and acrylic acid are investigated at pH 5 and pH 2. When the penultimate effects are not important and under steady state conditions, the copolymerization is governed by the well-known Mayo–Lewis equation.[2]

$$\frac{d[m_A]}{d[m_B]} = \left(\frac{[m_A]}{[m_B]}\right)\left(\frac{r_A[m_A] + [m_B]}{[m_A] + r_B[m_B]}\right) \quad (1)$$

Here, $[m_A]$ and $[m_B]$ are the monomer concentrations. The reactivity ratios r_A and r_B are defined as the ratios of the propagation rate constants, $r_A = k_{AA}/k_{AB}$ and $r_B = k_{BB}/k_{BA}$. Precise determination of reactivity ratios for various monomer pairs is important for predicting the behavior of the materials obtained by their copolymerization. When one or both of the comonomers are ionic, the reactivities depend strongly on the reaction medium, especially its pH and ionic strength.

Because of extensive usage of acrylic acid and acrylamide homo and copolymers in industry, there are many published works about this system.[3–9] The most recent study was performed by Wandrey and coworkers,[10,11] where sequential sampling method was applied and the pH ranged from 2 to 12 at 40°C. The basic method of Kelen and Tüdös was used. Cited results are given in Table I. They show considerable amount of scatter.

More recent monitoring techniques allow data to be obtained continuously during the reaction.[12–19] In

Correspondence to: H. Çatalgil-Giz (catalgil@itu.edu.tr).
Contract grant sponsor: I.T.Ü. Research Fund; contract grant numbers: 1673, and 1653.
Contract grant sponsor: TUBITAK;contract grant number: TBAG 2174 (102T060).
Contract grant sponsor: TUBITAK-BDP.

TABLE I
pH Dependence of Reactivity Ratios

pH	r_{Aam}	r_{Aac}	Reaction conv (%)	Reference
6.25	1.32 ± 0.12	0.35 ± 0.03	< 10	3
6	0.85 ± 0.62	0.33 ± 0.20	34–77	7
5.3	1.83	0.51	30–40	10
2.17	0.48 ± 0.06	1.73 ± 0.21	< 10	3
2	0.25 ± 0.36	0.92 ± 0.82	28–70	7
1.8	0.54	1.48	30–40	10
2	0.16 ± 0.04	0.88 ± 0.08	80–90	This work
5–6	1.88 ± 0.17	0.80 ± 0.07	80–90	This work

these techniques, a large amount of data are obtained for each experiment resulting in more accurate determination of reaction parameters.

In this work, acrylamide/acrylic acid copolymerization is studied by the automatic continuous online monitoring of polymerization (ACOMP) method, which has recently been further developed to encompass copolymerization reactions. Two sets of reactions were conducted at pH 5 and pH 2. The experiments were monitored on-line and the data were analyzed by a recent EVM type calculation method developed for use on data obtained by on-line monitoring.[20]

EXPERIMENTAL

ACOMP instrumentation

The automatic continuous online monitoring of polymerization (ACOMP) technique itself and its application to copolymerization have been adequately described,[19] but is undergoing constant improvement. In this application, a small amount of reactor material was continuously removed from the reactor by an Agilent isocratic pump and mixed at high pressure with a much larger volume of solvent drawn by another similar pump.

Two individual pumps and high-pressure mixing was preferred over a single pump and low-pressure mixing to overcome the tendency of the pump to draw more from the solvent reservoir as the viscosity of the reactor increased with conversion.[19] Still, it was necessary to terminate the reaction when the increase of viscosity of the reactor solution caused the reactor-side pump to de-prime. Hence, 100% conversion was not achieved in the reactions and the conversion typically ranged from 75 to 90%.

The diluted polymer solution was then passed through a train of detectors comprising a light scattering (LS) detector, a single capillary viscometer (Validyne differential pressure sensor) and a Shimadzu SPD-10AV ultraviolet spectrophotometer (UV). Data gathering and analysis software were developed in-house.

Materials

Acrylamide (Aam) and Acrylic acid (Aac) were used as received from Aldrich. Water was deionized and filtered by a 0.22 μm filter in a Modulab UF/UV system. The initiator was 4,4′-Azo bis (4-cyanovaleric acid) (ACV, Aldrich) and used as received. Sodium hydroxide (Aldrich) was used to set the pH and 0.1*M* NaCl (Aldrich) solution was used as the carrier solvent.

Polymerization

Before the polymerization reaction, the carrier solvent was pumped through the detector train to obtain the baseline of each instrument. After stabilization, the comonomer mixture containing the Aam and Aac at predetermined pH was pumped at a flow rate of 0.06 mL/min from the reactor and diluted with a flow of 1.94 mL/min of the carrier solvent. These flow rates from the reactor and the solvent reservoir were maintained throughout the entire experiment. The diluted solution always reached the detector train at 25°C, regardless of the reactor temperature.

TABLE II
Parameters of the Copolymerization Reactions

Exp code	Aac (%)	C_{Aac} (mol/L)	C_{Aam} (mol/L)	C_{NaOH} (mol/L)	C_{ACV} (10^{-3} mol/L)	$pH_{at\ 60°C}$	$pH_{after\ initiator}$	pH_{final}
I	0	–	0.47164	0.0025	8.917	8.30	5.20	5.08
II	10	0.04764	0.42289	0.04682	8.921	7.56	4.95	5.14
III	23	0.11261	0.37585	0.09369	8.919	7.80	5.01	5.23
IV	30	0.14135	0.32929	0.14102	8.917	7.34	4.82	5.41
V	50	0.23506	0.23523	0.23521	8.916	7.37	5.02	5.67
VI	70	0.33039	0.14181	0.32851	8.920	7.20	5.10	6.62
VII	76	0.35736	0.11291	0.35688	8.916	7.20	5.20	6.68
VIII	90	0.42455	0.04732	0.42755	8.921	7.26	5.31	7.16
IX	100	0.46536	–	0.46534	8.920	7.22	5.29	7.41
X	50	0.23506	0.23523	–	8.925	2.22	1.58	2.34
XI	70	0.32877	0.14112	–	9.004	2.41	1.59	2.87

Reaction temperature is $T = 60°C$.

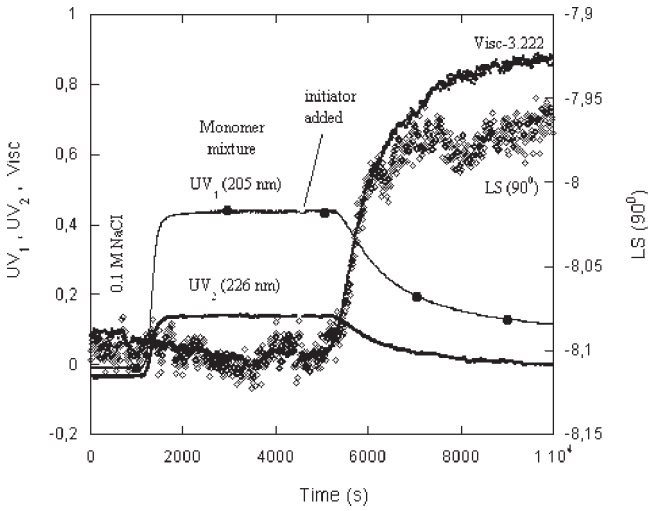

Figure 1 ACOMP data for reaction VI with 70% Aac and 30% Aam, at pH 5.

At the beginning of the reaction, reactor was purged for 30 min with N_2 and then was lowered into a temperature-controlled bath at 60°C. Reaction was initiated by adding the ACV in powder form. After adding the initiator, the pH was measured. The solution was magnetically stirred during the reaction. The amounts used, pH's measured at the beginning of the experiment, after the initiator addition, and at the end of reaction are given in Table II. Monitoring procedure was similar to Ref. 19. However, two UV absorption measurements at 205 and 226 nm were used in the monitoring conversion of the monomer to polymer.

Figure 1 shows the ACOMP data for the 30% Aam/70% Aac reaction at pH 5, where each step is indicated. They are the baseline stabilization period, the baseline of pure monomer, the point of initiator addition, and the polymerization period. The two UV signals increase during the pure monomer suction period, whereas the LS and viscosity do not change. During polymerization, the loss of the double bonds of each comonomer as it incorporates into polymer leads to (differentially) decreasing UV absorption in both bands, while the viscosity and LS signals increase with increasing polymer concentration.

Determination of comonomer and polymer concentrations from ACOMP

The concentrations of the two comonomers in their monomeric form as well as their concentrations incorporated into polymer are computed from the raw UV data. Throughout this work, Aam will be taken as monomer A and Aac as B. The absorbances of the initiator at these wavelengths can be neglected when compared with the absorbances of the monomers at the same wavelengths. Therefore, the UV voltage, V_{UV} at a specific wavelength is composed of the signals from the four species:

$$V_{\mathrm{UV}} = s\left(\frac{\partial V_{\mathrm{UV}}}{\partial [m_A]}[m_A] + \frac{\partial V_{\mathrm{UV}}}{\partial [p_A]}[p_A] + \frac{\partial V_{\mathrm{UV}}}{\partial [m_B]}[m_B] + \frac{\partial V_{\mathrm{UV}}}{\partial [p_B]}[p_B]\right) \quad (2)$$

where $[m_A]$ and $[p_A]$ are the monomer and polymer concentrations (in monomols) in the reactor of species A, and likewise for $[m_B]$ and $[p_B]$. The dilution ratio is $s = 0.06/2.00$. The ratio of the absorption coefficients of Aam and Aac is 1.62 at 205 nm, namely, wavelength 1 and 10.01 at 226 nm, wavelength 2. The nonequality of these ratios results in the linear independence of the two relations obtained by the application of eq. (2) to the measurements at these wavelengths.

UV absorption measurements are combined with the conservation equations,

$$[p_A] + [m_A] = [m_A]_0 \quad (3)$$

where $[m_A]_0$ is the monomer A concentration at the beginning of the reaction. A similar relation holds for monomer B. Here, the increase of the density of the reaction medium with conversion is neglected, as this effect is very small in dilute solution polymerization.

The two monomer concentrations are obtained from the observed UV absorbances via,

$$U_k^+ = \mathrm{UV}_{k_{\mathrm{signal}}} - \mathrm{UV}_{k_{\mathrm{baseline}}} - \frac{\partial V_{\mathrm{UV}_k}}{\partial [p_A]}[m_A]_0 - \frac{\partial V_{\mathrm{UV}_k}}{\partial [p_B]}[m_B]_0 \quad (4)$$

Here, $\mathrm{UV}_{\mathrm{signal}}$ and $\mathrm{UV}_{\mathrm{baseline}}$ are the voltages recorded during data gathering and the baseline voltage when pure solvent is passing through the detectors and the index k is 1 for measurements at wavelength 1 and 2 otherwise.

$$[m_A] = (\Delta U_{2B} U_1^+ - \Delta U_{1B} U_2^+)/\det \quad (5a)$$

$$[m_B] = -(\Delta U_{2A} U_1^+ - \Delta U_{1A} U_2^+)/\det \quad (5b)$$

where

$$\Delta U_{kA} = \frac{\partial V_{\mathrm{UV}_k}}{\partial [m_A]} - \frac{\partial V_{\mathrm{UV}_k}}{\partial [p_A]} \quad (5c)$$

ΔU_{kB} are defined similarly and the determinant det is given by,

$$\det = \Delta U_{1A}\Delta U_{2B} - \Delta U_{1B}\Delta U_{2A} \quad (5d)$$

The analysis of the UV data, according to the above scheme, yields a continuous record of the monomer concentrations $[m_A]$ and $[m_B]$, and the concentrations of A and B units in the copolymer $[p_A]$ and $[p_B]$.

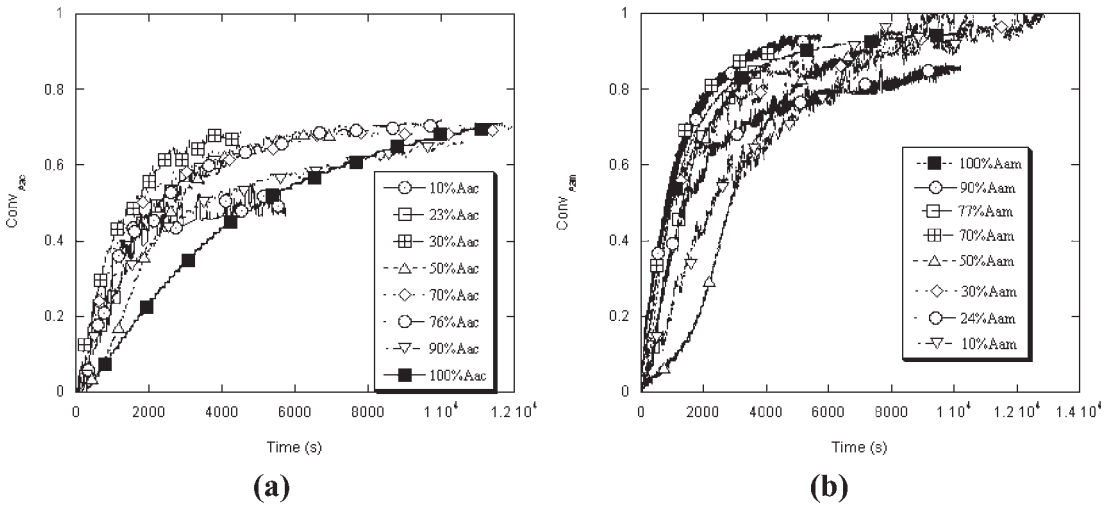

Figure 2 (a) Conversion of Aac for several reactions at pH 5. (b) Conversion of Aam for several reactions at pH 5.

Conversions of Aac and Aam for the reactions at pH 5 are shown in Figure 2(a,b), respectively. Figure 3 shows analogous results for the experiments performed at pH 2.

Nonlinear fit procedure

A recent EVM, developed especially for online data[19,20] is adapted for two UV measurements at different wavelengths.

To obtain the reactivity ratios, the data are fitted to a numerical solution of the copolymerization eq. (1) of the form

$$[m_A]_{\text{the}} = f([m_B], [m_A]_0, [m_B]_0, r_A, r_B) \quad (6)$$

where $[m_A]_{\text{the}}$ is the ''theoretical'' concentration of monomer A at the ith data point of the jth experiment, corresponding to a measured concentration of the other monomer $[m_B]_{ij}$, initial concentrations $[m_A]_{0j}$, and $[m_B]_{0j}$ and the reactivity ratios r_A and r_B.

This equation can be written as

$$Q_{ij} = [m_A]_{ij} - f([m_B]_{ij}, [m_A]_{0j}, [m_B]_{0j}, r_A, r_B) = 0 \quad (7)$$

where Q is a measure of the ''distance'' of the theoretical $[m_A]_{\text{the}}$ from the experimental $[m_A]$. The χ^2 value corresponding to this set of parameters, r_A and r_B, is then obtained by summing the ratio of the square of this distance to the variation of Q at that data point, $\text{Var}Q_{ij}$.

$$\chi^2(r_A, r_B) = \sum_{j=1}^{n(\text{exp})} \sum_{i=1}^{n(\text{data})_j} Q_{ij}^2/\text{Var}(Q_{ij}) \quad (8)$$

The sum runs over all data points in all experiments. In these experiments, only data recorded up to 50% conversion of the faster monomer was used.

The error terms that contribute to the variation arise from the UV measurements, their baseline values, and the calibration constants. Measurements of the initial concentrations cause additional errors. However, in these experiments, the error structure is dominated by UV measurement errors. Thus, the variations of the monomer concentrations and their covariance are given by,

$$\text{Var}(Q) = \text{Var}([m_A]) + \text{Var}([m_B])$$

$$\text{Var}([m_A]) = \{(\Delta U_{2B})^2\text{Var}(U_1^+) + (\Delta U_{1B})^2\text{Var}(U_2^+)\}/\det^2$$

$$\text{Var}([m_B]) = \{(\Delta U_{2A})^2\text{Var}(U_1^+) + (\Delta U_{1A})^2\text{Var}(U_2^+)\}/\det^2$$

$$\text{Covar}([m_A], [m_B]) = \{(\Delta U_{2A})(\Delta U_{2B})\text{Var}(U_1^+) + (\Delta U_{1A})(\Delta U_{1B})\text{Var}(U_2^+)\}/\det^2$$

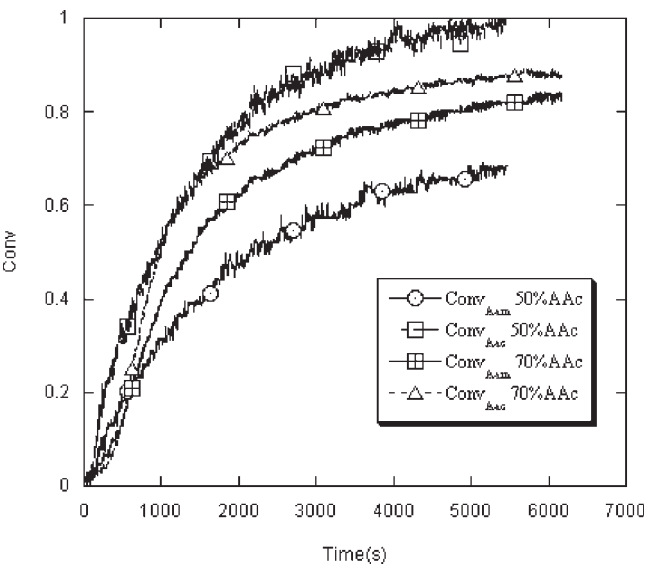

Figure 3 Monomer conversion in the experiments performed at pH2.

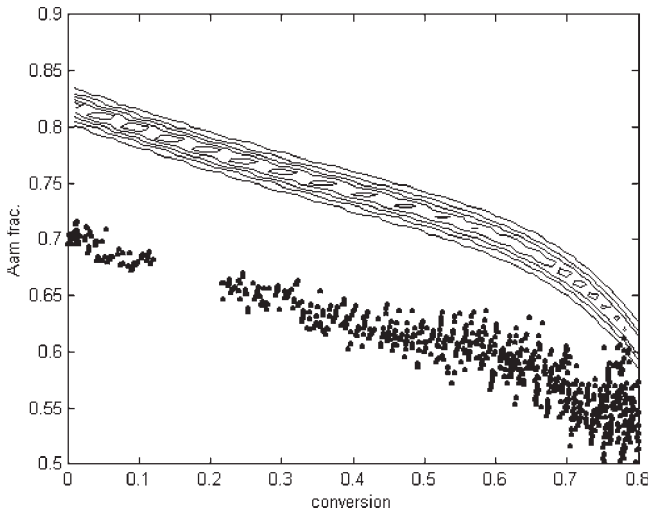

Figure 4 The compositional drift during the reaction at pH 5 with 70% initial Aam content.

where

$$\mathrm{Var}(U_1^+) = \delta(\mathrm{UV}_{1\mathrm{signal}})^2 + \delta(\mathrm{UV}_{1\mathrm{baseline}})^2$$
$$\mathrm{Var}(U_2^+) = \delta(\mathrm{UV}_{2\mathrm{signal}})^2 + \delta(\mathrm{UV}_{2\mathrm{baseline}})^2$$

Since, not just the best fit parameters, but the statistically acceptable part of the parameter space is important, the whole parameter space was scanned by repeating the procedure for each pair of r_A and r_B within the search zone. The χ^2 contours were plotted as functions of the reactivity ratios for each individual experiment at the studied pH.

The contours for the combined results of all experiments at that pH are also plotted. They show the acceptable region in the r_A, r_B parameter space.

RESULTS AND DISCUSSION

Composition drift

As the more reactive monomer incorporates into the copolymer faster, the feed composition drifts during the reaction. This drift is an undesirable effect and must be compensated for in-batch methods. However, in on-line methods, the composition drift is continuously monitored and it can be used to give a rough idea of the reactivity ratios before any numerical computation is performed.

The composition of the material incorporating instantaneously into copolymer is found from the instantaneous monomer composition and its derivative.

Let f_{Aam} be the instantaneous Aam fraction in the feed mixture when the conversion is x, and F_{Aam} be the Aam fraction in the amount dx that incorporates into the copolymer at this instant. This dx contains $dx(F_{\mathrm{Aam}})$ amount of Aam and $dx(1 - F_{\mathrm{Aam}})$ of Aac. If $F_{\mathrm{Aam}} \neq f_{\mathrm{Aam}}$, the composition drifts. When the monomer composition is continuously monitored, f_{Aam} and its derivative with respect to conversion can be used to obtain the composition of the material joining the copolymer instantaneously as,

$$F_{\mathrm{Aam}} = f_{\mathrm{Aam}} - (1 - x)\frac{df_{\mathrm{Aam}}}{dx} \quad (9)$$

The f_{Aam} versus conversion data in reaction IV with 70% initial Aam content at pH 5 are given in Figure 4. The dots are the experimental f_{Aam} data and the F_{Aam} contours are obtained by applying the above-mentioned formula to the best fit curve of the experimental data, and then using the Stockmayer et al. distribution function[21] to flesh it out. The Aam fraction is greater in polymer than in monomer, indicating that it is entering the reaction at a rate higher than its fraction in the monomer mixture. As a result, the Aam fraction is decreasing both in monomer mixture and in the instantaneous copolymer formed. The fact that Aam fraction is drifting down at this initial composition shows that $r_{\mathrm{Aam}} > r_{\mathrm{Aac}}$ at pH 5.

At pH 2, the Aac is the more active monomer and it is depleted faster. Composition drift during the reaction with 70% Aac content at pH 2 is given in Figure 5. The Aac content of the unreacted monomer mixture is decreasing throughout the reaction, indicating that the Aac is entering the reaction at a faster rate. This is because of the ionic nature of Aam, which is protonated at pH 2.[22] As a result, the Aac fraction is higher in the polymer than in the reaction mixture.

Reactivity ratios

Figure 6(a,b) show the superposition of χ^2 contours for the individual experiments at pH 5 and the combined results of all experiments at this pH.

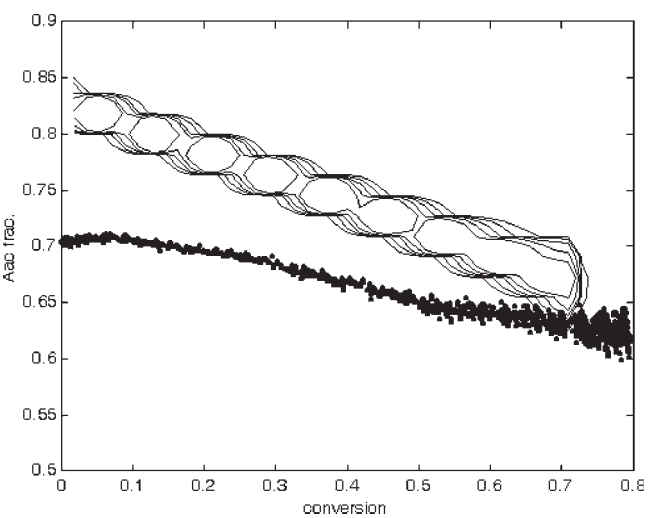

Figure 5 The compositional drift during the reaction at pH 2 with 70% initial Aac content.

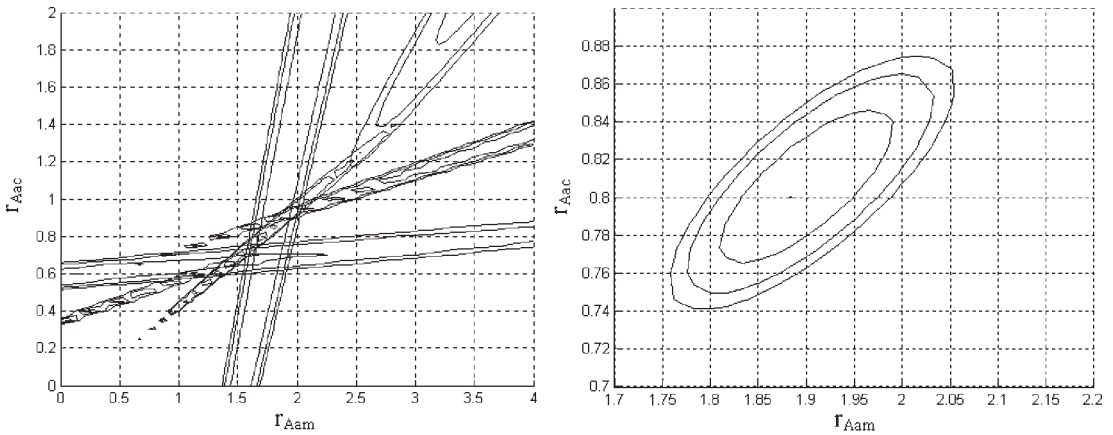

Figure 6 (a) The reactivity contour maps for the individual experiments conducted at pH 5. (b) The reactivity contour maps for combined results at pH 5.

The valleys in Figure 6(a) show the 1, 2, and 3 σ confidence regions for the individual experiments. Note that they do not intersect exactly at the same point. This is because one of the experimental conditions, namely the ionic strength, which depends on the Aac concentration, is not the same in each experiment; in fact, it changes with conversion, during the experiment itself. For this reason, the combined confidence region given in Figure 6(b) represents the cumulative average over the conditions valid during the whole experiment series.

Corresponding figures for pH 2 were shown in Figure 7(a,b), respectively. Again, the contours in Figure 7(a) represent the average of the conditions during individual experiments, and the Figure 7(b), the cumulative average over both experiments.

The reactivity ratios at pH 5 are found as $r_{\mathrm{Aam}} = 1.88 \pm 0.17$ and $r_{\mathrm{Aac}} = 0.80 \pm 0.07$ from Figure 6(b), and the reactivity ratios are found as $r_{\mathrm{Aam}} = 0.16 \pm 0.04$ and $r_{\mathrm{Aac}} = 0.88 \pm 0.08$ at pH 2 from Figure 7(b).

The dramatic shift in the reactivity ratios with pH had been noted in the literature as shown in Table I. On the other hand, numerical values obtained by various authors show considerable scatter.

The strong pH dependence of the Aam reactivity is not surprising, as ionic strength of the reaction medium determines to what extent the charge on the macro radical is screened.

We would expect the change in the Aac reactivity to be larger too. Previous literature results show a greater increase in r_{Aac} with decreasing pH. However, in our experiments, the increase was much more limited. Even so, as the reactivity of Aam decreases almost to zero at pH 2, the Aac enters the reaction at a much faster rate.

The Henderson-Hasselbach[23] equation with pKa taken as 4.26[11] for Aac predicts more than 99% ioniza-

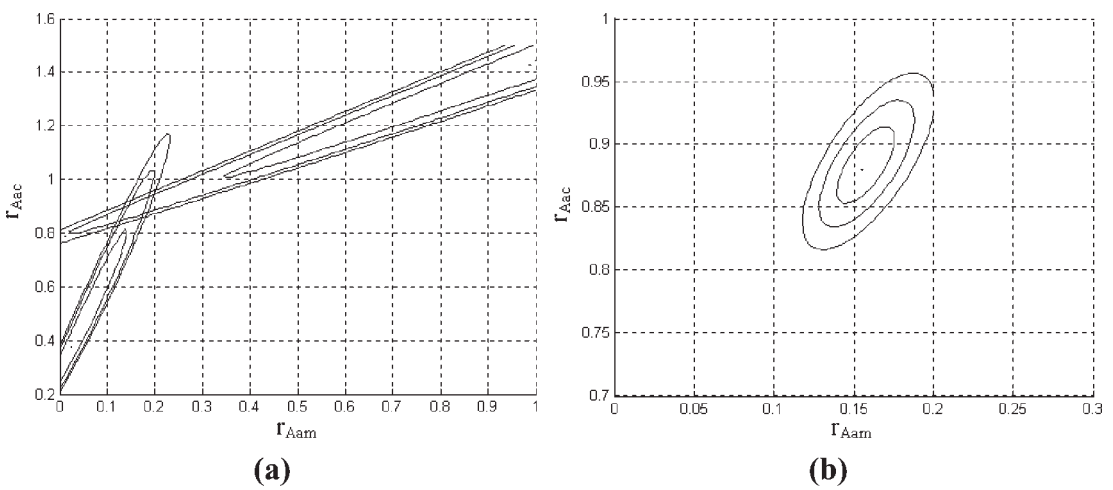

Figure 7 (a) The reactivity contour maps for the individual experiments conducted at pH 2. (b) The reactivity contour maps for combined results at pH 2.

tion at pH 5. At this pH, the acid units in the chain are effectively screened by the Na^+ ions, which were added to the system to set the pH at the beginning of the reaction. Therefore, sodium acrylate units can be considered as uncharged. At pH 2, the ionization degree for Aac is very low, that is, only 0.05%. The proton is tightly bonded to the acid group, and Aac groups can be considered as neutral at pH 2. This is the similarity of Aac at pH 2 and pH 5 and their reactivity ratios at these pH's resulted in similar values.

On the other hand, Aam is neutral at pH 5 but it is known to be protonated at pH 2.[22] The difference in the reactivities of this monomer at this pH is no doubt a consequence of the protonation of the Aam at pH 2. The electrostatic repulsion between the macro radical and the charged monomer is likely to be the cause of the low reactivity of the Aam at pH 2.

CONCLUSIONS

ACOMP has been used for the first time to monitor the synthesis of polyelectrolytic copolymers of Aac and Aam. At pH 5, acrylamide was the more active monomer, and Aam content correlates with the reaction rate. At pH 2, the reverse is true.

The numerical values for the reactivities differ in all of the studies. Differences in the reactor temperature, use of linear or nonlinear analysis methods, and using low conversion versus high conversion results are some of the factors contributing to the spread in the results. Since, the behavior of polyelectrolytes depend so strongly on the reaction medium, changes in the properties of the medium, such as its pH, ionic strength, and viscosity, during the reaction also effect the results.

However, low conversion work is purer because of the intrinsic value of the results, high-conversion work is more relevant to practical applications. On-line data acquisition techniques, which give hundreds or even thousands of points throughout an experiment, provide much better statistics. They are also useful to determine whether the measured parameters remain constant during the reaction. That is, if low-conversion results lead to different values than high-conversion results, one would conclude that the measured parameters are not constant but evolve during the reaction. For these reasons, on-line methods give much more information from each reaction.

The authors are grateful to Prof. Dr. W. Reed, Tulane University (USA), for allowing the full use of his laboratory during this work.

References

1. Förster, S.; Schimidt, M. Adv Polym Sci 1995, 120, 51.
2. Mayo, F. R.; Lewis, F. M. J Am Chem Soc 1944, 66, 1594.
3. Cabaness, R.; Yen-Chin-Lin, T.; Parkanyi, C. J Polym Sci Part A-1: Polym Chem 1971, 9, 2155.
4. Mast, C. J.; Cabaness, W. R. J Polym Sci Polym Lett Ed 1973, 11, 161.
5. Wang, M. C.; Cabaness, W. R. J Polym Sci Polym Lett Ed 1975, 13, 369.
6. Shawki, S. M.; Hamielec, A. E. J Appl Polym Sci 1979, 23, 3155.
7. Ponratnam, S.; Kapur, S. L. Makromol Chem 1977, 178, 1029.
8. Kurenkov, V. F.; Myagchenkov, V. A. Eur Polym J 1980, 16, 1229.
9. Truong, N. D.; Galin, J. C.; Francois, J.; Pham, Q. T. Polymer 1986, 27, 467.
10. Rintoul, I.; Wandrey, C. Polymer 2005, 46, 4525.
11. Rintoul, I.; Wandrey, C. Macromolecules 2005, 38, 8108.
12. Florenzano, F. H.; Strelitzki, R.; Reed, W. F. Macromolecules 1998, 31, 7226.
13. Strelitzki, R.; Reed, W. F. J Appl Polym Sci 1999, 73, 2359.
14. Norwood, D. P.; Reed, W. F. Int J Polym Anal Char 1997, 4, 99.
15. Grassl, B.; Alb, A. M.; Reed, W. F. Macromol Chem Phys 2001, 12, 2518.
16. Giz, A.; Çatalgil-Giz, H.; Brousseau, J.-L.; Alb, A. M.; Reed, W. F. Macromolecules 2001, 34, 1180.
17. Reed, W. F. Macromolecules 2000, 33, 7165.
18. Chauvin, F.; Alb, A. M.; Bertin, D.; Tordo, P.; Reed, W. F. Macromol Chem Phys 2002, 203, 2029.
19. Çatalgil-Giz, H.; Giz, A.; Alb, A. M.; Öncül-Koç, A.; Reed, W. F. Macromolecules 2002, 35, 6557.
20. Sünbül, D.; Çatalgil-Giz, H.; Reed, W.; Giz, A. Macromol Theory Simul 2004, 13, 162.
21. Stockmayer, W. H.; Moore, L. D.; Fixman, M.; Epstein, B. N. J Polym Sci 1955, 16, 517.
22. Breslow, R. Organic Reaction Mechanism; Benjamin: New York, 1969; p 17.
23. Alexandrowicz, Z.; Katchalsky, A. J Polym Sci Part A-1: Polym Chem 1963, 1, 3231.